

# Robust Data-Optimized Stochastic Analog-to-Digital Converters

Thinh Nguyen, *Member, IEEE*

**Abstract**—The majority of Analog-to-Digital converters (ADC) are designed without taking into consideration the distribution of input signal. In this paper, we present a novel ADC architecture that is optimized for a given input signal's statistics. The new robust data-optimized stochastic flash (RDSF) ADC achieves robustness and high accuracy by employing (a) a large number of 1-bit quantizers operating in parallel with an additive noise and (b) a novel probability density transform (PDT). We demonstrate the performance gain of the RDSF over the conventional flash ADC using simulations and theoretical analysis.

**Index Terms**—Data converters, quantization

## I. INTRODUCTION

Conventional flash A-D converters (ADC) are implemented using a number of 1-bit comparators connecting together in series [1]. When a particular comparator fails, a certain output value will never be obtained, thus reducing the robustness of an ADC. In addition, a conventional flash ADC does not take into account the statistics of input signal, and therefore, its performance is not optimal. Knowing the statistics of the input signal is beneficial. For example, if the input signal is known to concentrate around a certain value  $x$ , one can design an ADC that has small quantization step sizes in the regions around  $x$ , and larger quantization step sizes in other regions [2]. This design effectively reduces the quantization errors for most of the input values, resulting in small average quantization error. However, this approach requires a non-uniform quantizer which has higher circuit implementation complexity than that of a simple uniform quantizer. In this paper, we extend the works of McDonnell et al. [3] to design a simple, robust data-optimized stochastic flash (RDSF) ADC that achieves high accuracy using only 1-bit quantizers and an additive noise. We now begin with a few related work.

## II. RELATED WORK

The idea of adding random noise to the input signal to reduce noise has been explored by many researchers over the years. In the image processing community, researchers have been employing dithering techniques in which random noise is added to the image before quantization in order to reduce the quantization errors. For example, to improve the PCM coding [4] of an image, Roberts proposed the pseudo noise technique - a method that removes the signal dependence of the quantization noise [5]. Similarly, research in sensor networks employ multiple sensors to collaboratively estimate

data under noisy environment, and thus, there is no need to add an artificial noise [6].

The stochastic framework on which this paper is based on, has its root in the stochastic resonance (SR) phenomenon in physics. SR phenomenon occurs when the combination of a small periodic signal and a large noise drives a nonlinear system to switch between the two stable states. With the appropriate value of noise, the period of the state switching equals to the period of the small signal. Thus, weak information signal can be amplified and optimized by the assistance of noise [7]. Recently, Stocks et al. proposed Suprathreshold Stochastic Resonance (SSR) using multilevel thresholds which can extend the dynamic range of an input signal [8]. Subsequently, Rousseau et al. presented a detail analysis on the SNR performance of such SSR systems [9]. Most similar to our work is that of McDonnell et al. [10][3]. In this work, McDonnell et al. provided a framework for designing ADC using SSR<sup>1</sup>. Incidentally, our basic stochastic ADC is a special case of SSR. On the other hand, we propose a new RDSF ADC based on a probability density transform (PDT) technique to increase the converter's accuracy. The PDT technique first transforms an input signal into a high variance signal. Next, a random independent noise is added to it, and the resulted signal is quantized by a set of simple 1-bit uniform quantizers. Finally, an digital output is estimated as the average of all the 1-bit values from the quantizers. The performance of the PDT technique depends on the probability density distribution of the input signals. While our proposed approach relies on prior knowledge about the data distribution, this prior knowledge can be imprecise. In particular, we assume to know only the distribution type of the input signal, not its specific distribution parameters. We now describe the architecture of a basic RSF ADC.

## III. RSF ADC

Figure 1 shows the architecture for the basic stochastic flash ADC proposed by Stocks and McDonnell et al. in [8][3]. This structure consists of a set of  $M$  coarse quantizers, e.g., 1-bit comparators, operating in parallel. Independent and identically distributed noise is then added to the input signal, and the results are fed to the quantizers. The estimated signal is then the average of all the  $M$  digital outputs from the  $M$  quantizers. In [3], the thresholds of different comparators are different in order to create a  $M$  different levels. We note that designing circuits having a large number of different thresholds at fine

Manuscript received July 25, 2005; revised August 06, 2006.

Thinh Nguyen is with the Department of Electrical Engineering and Computer Science at Oregon State University.

<sup>1</sup>The idea of stochastic flash converter was proposed independently in 1992 by Ian Galton, however, the author did not publish the idea.

quantization levels is a challenging task. Thus, our basic RSF ADC is a special case of SSR where the thresholds of all comparators are identical and equal to 0. Assuming that the output from each quantizer is either 1 or -1, then the maximum number of different output values is  $M + 1$ . Hence, this design still operates probabilistically as an  $M + 1$ -level quantizer, and the output's accuracy is on the order of  $\sqrt{M}$ . The performance

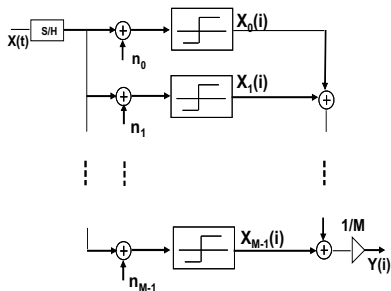


Fig. 1. Diagram of a stochastic flash ADC consisting of  $M$  1-bit quantizers. Uncorrelated noise is added to the input signal before quantization. The accurate output is obtained by averaging the  $M$  digital outputs.

of this RSF ADC depends on the noise characteristics. Clearly, the noise samples need to be independent and identically distributed in order for this design to work. Furthermore, the noise distribution plays a crucial role in the performance of the RSF ADC. In this paper, we only consider the performance of the RSF ADC under the addition of a uniform noise since the circuits for generating uniformly distributed analog noise have been implemented by many researchers [11]. We derived the following result:

**Theorem 1:** If an input signal  $x$  and an additive noise  $n_i$  are uniformly distributed in the intervals  $[-\alpha, \alpha]$  and  $[-\beta, \beta]$ , respectively, with  $\beta \geq \alpha$ , then the quantization error power  $E$  using the estimator  $\hat{x} = \frac{\alpha}{M} \sum_{i=1}^M \text{sign}(x + n_i)$  is

$$E = \frac{\alpha^2}{3} - \frac{2\alpha^3}{3\beta} + \frac{(M-1)\alpha^4}{3M\beta^2} + \frac{\alpha^2}{M}. \quad (1)$$

**Proof:** See the Appendix.

Theorem 1 states that the quantization error power is inversely proportional to  $M$ . This agrees with our intuition that a larger  $M$  leads to a smaller quantization error. Also, when a few quantizers fail, the quantization error will increase only slightly, resulting in high robustness.

**Theorem 2:** If an input signal  $x$  has a pdf  $p(x)$  with  $x$  symmetrically distributed over  $[-\alpha, \alpha]$  and an additive noise is independent and uniformly distributed over  $[-\alpha, \alpha]$ , then the quantization error power  $E_g$  is

$$E_g = \frac{\alpha^2 - \text{Var}(x)}{M}. \quad (2)$$

**Proof:** (outline): Using the same derivation as in the proof of Theorem 1, setting  $\beta = \alpha$ , and leaving the integration intact, we obtain the desired result. ■

Theorem 2 indicates that an input signal with high variance will result in a lower quantization error. This fact will be used to design the probability density transformation (PDT) technique in the RDSF ADC.

## IV. RDSF ADC

In this section, we first discuss the framework of RDSF ADC and the properties of a good probability density transform. We then propose a good generic transform function and provide the theoretical performance of the proposed RDSF ADC for the input signals having Gaussian-like distributions.

**Framework.** Figure 2 shows the diagram for the proposed RDSF ADC. The input signal is first transformed to result in a large variance signal. Next, the transformed signal is fed to the basic RSF ADC. Finally, the digital output signal from the RSF ADC is inversely transformed to obtain the correct digital output. Clearly, not every input signal needs to

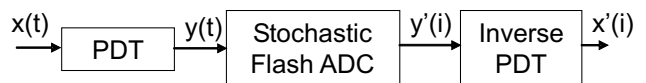


Fig. 2. Diagram of the RDSF ADC. The input signal is transformed before feeding to the basic RSF ADC. The digital output of RSF ADC is transformed back to the correct digital signal.

be transformed. If the distribution of an input signal already has a high variance, no transformation is needed. Figure 3 shows three canonical shapes of typical distributions with zero means and different variances. Ranking in the order from lowest to highest variances are Gaussian-like, uniform, and bimodal-like signals. Since the proposed RSF ADC performs better for the input signals having large variances (bimodal-like distributions), the goal of the PDT is to transform the probability density function of a given input signal into a bimodal-like distribution.

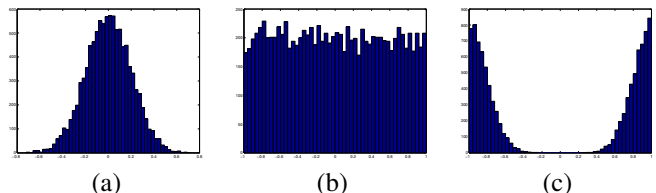


Fig. 3. (a) A Gaussian-like distribution has small variance; (b) A uniform-like distribution has medium variance; (c) A bimodal distribution has large variance.

**PDT.** The transform function is critical for the effectiveness of the PDT framework. As such, we advocate the following requirements and properties for a good PDT.

1. *The transform must be invertible.* This requirement is obvious as one must be able to get back the original signal.

2. *The transform must preserve the range of an input signal.* This requirement enables a practical circuit implementation with regard to power usage and reference voltage. Scaling up the input signal results in power increase, and changing the reference voltage within a circuit complicates the design.

3. *The transform must be designed such that the total quantization error of the reconstructed signal is smaller than that obtained by the basic RSF ADC.* We note that a transform function may produce a very small quantization error power for the transformed signal. However, when the transformed signal is converted back to the original signal using its inverse

transform, this small quantization error power might be amplified significantly, making the PDT framework ineffective. Our goal is to design a transform function such that (a) the quantization error reduces after the forward transform, and (b) does not amplify after the inverse transform. Given this transform, the overall quantization error using the RDSF ADC ( $x(t) - x'(i)$  in Figure 2) will equal to the quantization error of the transformed input signal ( $y(t) - y'(i)$ ), which will be smaller than the quantization error produced by the basic RSF ADC.

4. *Both forward and inverse transforms should be simple in order to be realized in analog and digital circuits.*

We now present a generic transform function called **Split and Shift (SAS)** to be used for Gaussian-like input signals. SAS meets all the above requirements/properties.

**Split and Shift (SAS).** The idea for SAS is simple. First, we note that a non-zero mean distribution can be easily transformed into a zero-mean distribution by simply subtracting the mean from the random variable. Hence, our description of SAS will be referred to a random variable  $x$  having zero mean and bounded between  $\pm\alpha$ . Taking advantage of the symmetry and the concentration of values around the mean of a Gaussian-like distribution, we perform the following operations to change a Gaussian-like distribution into a bimodal-like distribution. First, we split the  $pdf(x)$  of the Gaussian-like distribution into left and right halves ( $x < 0$  and  $x \geq 0$ ). Second, we move the left half to the right and the right half to the left by  $\alpha$ . Pictorially, the SAS operations change the pdf's shape of a signal in Figure 3(a) to Figure 3(c).

Mathematically, the SAS transform is described by

$$y = T(x) = \begin{cases} x + \alpha & \text{if } x < 0 \\ x - \alpha & \text{if } x \geq 0 \end{cases}, \quad (3)$$

and the corresponding inverse transform is

$$x = T^{-1}(y) = \begin{cases} y - \alpha & \text{if } y > 0 \\ y + \alpha & \text{if } y \leq 0 \end{cases}. \quad (4)$$

*Theorem 3: SAS transform has following properties:*

1. *It is invertible.*
2. *It preserves the range of the input signals.*
3. *It results in the quantization error of the transformed signal equals to the overall quantization error.*

*Proof:* Properties 1 and 2 are obviously true from the definitions of the forward and inverse transforms. For property 3, let us denote  $\Delta$  and  $\Delta'$  as the quantization error of the transformed signal and the original signal, respectively. We want to show that  $\Delta = \Delta'$ . Denote the transformed value as  $y = T(x)$  and the quantized transformed value as  $y'$ , then  $\Delta = y' - y$ . Similarly, denote the original input signal as  $x$  and the reconstructed input signal  $x' = T^{-1}(y')$ , then  $\Delta' = x' - x$ . Consider the case  $y' \leq 0$ , we have  $x' = T^{-1}(y') = y' + \alpha = y + \Delta + \alpha$ . Now,  $\Delta' = x' - x = (y + \Delta + \alpha) - (y + \alpha) = \Delta$ . A similar argument can be made for the case  $y' > 0$ . Hence  $\Delta = \Delta'$  for  $y \in [-\alpha, \alpha]$ . ■

Property 3 is important as the SAS inverse transform guarantees no error amplification. *In other words, the forward SAS transform helps reduce the quantization errors of the input*

*signals in the transformed domain, and these errors remain the same after the inverse SAS transform. Hence, using PDT technique results in smaller overall quantization errors.*

Based on Theorem 4, the SAS transform is a good PDT function since it satisfies the first three requirements above. We also note that the analog circuit for the forward SAS transform is simple (property 4) since it only involves adding and subtracting  $\alpha$  from the signal. Similarly, the inverse transform in the digital domain is also extremely simple. Hence, we believe that a practical realization of the RDSF ADC is possible. We now present the theoretical performance of the proposed RDSF ADC using SAS PDT.

*Theorem 4: Using the RDSF with a SAS transform, the quantization error power  $E$  of an input signal having Gaussian distribution with zero mean and variance  $\delta^2$  with  $\delta \ll \alpha$  is approximately*

$$E = \frac{\frac{2\sqrt{2}\alpha\delta}{\sqrt{\pi}}(1 - e^{-\frac{\alpha^2}{2\delta^2}}) - \delta^2}{M}, \quad (5)$$

where  $M$  is the number of 1-bit quantizers and  $[-\alpha, \alpha]$  is the cut-off range of the input signal.

*Proof:* See the Appendix.

## V. RESULTS AND DISCUSSIONS

In this section, we present the simulation and theoretical results on quantization noise power for the proposed RDSF converters under a variety of settings. In addition, we show *visually* the robustness of our proposed RDSF over the conventional flash ADC by using the RDSF converter to quantize the image data.

In our simulations, we use the Gaussian input signals with zero means, each having different standard deviations. The input signals are limited to the range  $[-1, 1]$  by thresholding all values outside of  $[-1, 1]$  to 1 or -1. Figure 4 shows the quantization error power of the RSF and the RDSF ADCs as a function of the standard deviations of the input signal. As expected, the quantization error power of the RDSF ADC is much smaller than that of an RSF ADC. The performance gap, however, decreases with the increase of the input signal's standard deviation. This phenomenon is plausible since, as the standard deviation increases, the shape of the probability density distribution of the input signal widens, whence, the SAS operations no longer produce two distinct lumps. Therefore, the PDT technique is less effective. At one extremity, the SAS operations on an uniform distribution will not reduce the quantization error.

Figure 4 also shows that, for the input signals with small variances, the simulated quantization error powers agree very well with the theoretical predictions from Theorem 4. However, as the variance of the input signal increases, the theoretical approximation in Theorem 4 fails since the condition  $\delta \ll \alpha$  no longer holds.

To quantify the performance of the proposed ADC for real data, we chose to quantize the Haar wavelet coefficients of natural images since they typically follow a Gaussian-like distribution. We first decompose the standard Camera and Lena images into wavelet coefficients. Next, the diagonal

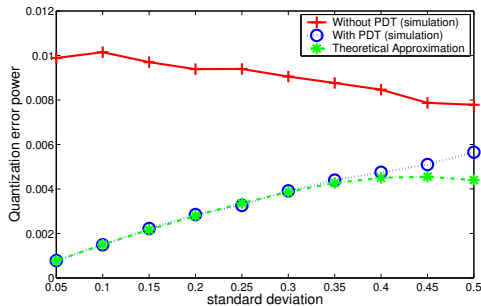


Fig. 4. Simulation and theoretical results on quantization error vs. std for RDSF ADC with Gaussian input signals.

wavelet coefficients at level 1 are first normalized to the range  $[-1, 1]$  and then quantized using RDSF ADC. Figure 5 shows the quantization error power as a function of the number of quantizers for the wavelet coefficients of the Camera and Lena images. As predicted, the quantization error decreases as the number of quantizers increases as observed with Gaussian-like input signals. The plots in Figure 5 also show that using PDT technique results in much smaller quantization errors than those obtained with the basic RSF ADC. To visually compare

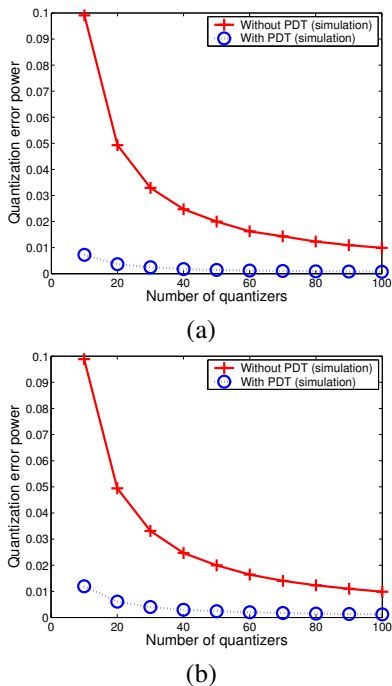


Fig. 5. Quantization error power for the quantized wavelet coefficients as a function of the number of 1-bit quantizers  $M$  for (a) the Camera and (b) the Lena images.

the robustness of the RDSF ADC and the conventional flash ADC, we quantize the wavelet coefficients of the Camera and Lena images using the conventional flash ADC and the RDSF ADC. The conventional flash ADC has 9 levels which requires 9 op-amps. From Theorem 2, in order to have the same quantization error, the number of quantizers for the stochastic flash needs to be  $81\sqrt{2} \approx 114$ . However, using the PDT, we observe empirically that only 40 quantizers are needed in the

RDSF ADC to obtain the same average quantization error. Both RDSF and conventional flash ADCs are then subject to a 10% failure rate. In other words, there are 1 and 4 quantizer failures in the conventional flash and the RDSF ADC, respectively. Figure 6(a) shows the original Camera image, Figure 6(b) shows the original wavelet coefficients of the Camera image while Figures 6(c) and 6(d) show the quantized wavelet coefficients resulted from conventional flash and the RDSF ADCs under failure conditions, respectively. The average quantization error powers for the RDSF and the conventional flash ADCs are 0.18 and 0.19, respectively. Although the average quantization error power of the RDSF ADC is slightly smaller than that of conventional flash, the main advantage of RDSF over conventional flash is its ability to diffuse the errors. This advantage is seen in the visual differences between Figures 6(c) and 6(d).

Compared to the original wavelet image in Figure 6(b), all the high intensity values are missing in Figure 6(c), noticeably along the tripod's leg and handle. This result is not surprising since, when a quantizer in the conventional flash fails, certain input signals can never be converted correctly. On the other hand, due to the stochastic nature of the RDSF ADC, its quantization error is distributed among different quantization levels, thus enabling a graceful degradation in the output quality.

**Comparisons with other ADCs.** The biggest disadvantage of the RDSF ADC is that the number of comparators is larger than that of the conventional flash, pipelined, and sigma-delta ADCs. The sigma-delta ADC has the smallest number of comparators, but it requires high oversampling rate. The pipelined ADC has the second smallest number of comparators, however, it is slow due to successive approximations. On the other hand, the RDSF is potentially the fastest one since the large resistor loads (in front of the op-amp) are not required due to identical reference voltages. This also makes the design of the RDSF very simple. Due to the large number of comparators, the RDSF probably makes sense only for ADCs with accuracy of 6-bit or less with the current technology. Despite of this disadvantage, the RDSF is most robust in harsh conditions, e.g. radiation exposure which can cause op-amp (comparator) failures.

## VI. ACKNOWLEDGMENT

We would like to thank Professor Gabor Temes and Professor Luca Luchese for the useful discussions. We also would like to thank the Center for Design of Analog and Digital Integrated Circuits (CDADIC) for the generous support of this project.

## VII. CONCLUSIONS

In this work, we have extended the existing stochastic framework for designing ADCs which incorporates the data statistics in order to (1) reduce the quantization errors and (2) to increase the robustness. We have presented simulation results and derived the theoretical performance for our proposed RDSF ADC. We have shown that the proposed RDSF ADC using the PDT technique can outperform the basic RSF ADC substantially.

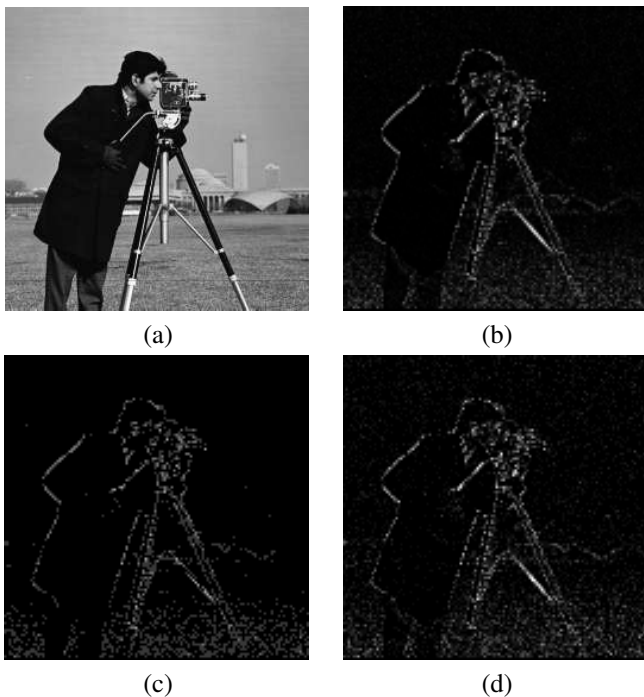


Fig. 6. (a) The original Camera image; (b) Original wavelet coefficients; (c) Quantized wavelet coefficients using the conventional flash ADC, and (d) Quantized wavelet coefficients using the RDSF ADC.

## REFERENCES

- [1] Razavi, *Principle of Data Conversion System Design*, IEEE Press, 1995.
- [2] T. Cover and J. Thomas, *Elements of information theory*, Wiley and sons, 1991.
- [3] M. McDonnell, N. Stocks, C. Pearce, and D. Abbott, "Analog to digital conversion using suprathreshold stochastic resonance," in *Proceeding of the SPIE*, 2005.
- [4] J. Lim and A. Oppenheim, "Reduction of quantization noise in pcm speech coding," *IEEE Transaction on Acoustic Speech Signal Processing*, pp. 107–110, Feb 1980.
- [5] J. Roberts, "Picture coding using pseudo-random noise," *IRE Transaction on Information Theory*, vol. 8, pp. 145–154, Jan 1962.
- [6] Z. Luo and J. Xiao, "Decentralized estimation in an inhomogeneous environment," in *ISIT*, 2004, p. 520.
- [7] L. Gammaitoni, P. Hanggi, P. Jung, and F. Marchesoni, "Stochastic resonance," *Reviews of Modern Physics*, vol. 70, no. 1, pp. 223–287, 1998.
- [8] N. Stocks, "Suprathreshold stochastic resonance in multilevel threshold systems," *Physical Review Letters*, vol. 84, no. 11, pp. 2310–2313, 2000.
- [9] D. Rousseau and F. Chapeau-Blondeau, "Suprathreshold stochastic resonance and signal-to-noise ratio improvement in arrays of comparators," *Physics Letters A*, pp. 280–290, 2004.
- [10] M. McDonnell, D. Abbott, and C. Pearce, "A characterization of suprathreshold stochastic resonance in an array of comparators by correlation coefficient," *Fluctuation and Noise Letters*, pp. 213–228, 2002.
- [11] G. Cauwenberghs, "Delta-sigma cellular automata for analog vlsi random vector generator," *IEEE Transactions on Circuits and Systems-II: Analog and digital signal processing*, vol. 46, no. 3, pp. 240–250, March 1999.
- [12] R. Yates and D. Goodman, *Probability and stochastic processes, 2nd edition*, Wiley and Sons, 2005.

## APPENDIX I PROOF OF THEOREM 1

Let us denote the probability density function of the input signal  $x$  as  $p(x)$ , the quantization error as  $e$ , the additive noise as  $n$ , and the number of 1-bit quantizers as  $M$ . We assume

that  $x \in [-\alpha, \alpha]$  and  $n \in [-\beta, \beta]$  with  $\beta \geq \alpha$ . Then, the quantization error is computed as

$$e = x - \frac{\alpha}{M} \sum_{i=1}^M \text{sign}(x + n_i), \quad (6)$$

where  $n_i$  is the noise random sample for each of the  $M$  quantizers. Note that  $\text{sign}(x + n_i)$  is either 1 or -1, whence we must scale the estimate by a factor of  $\alpha$  to match the input signal. By letting  $k = \sum_{i=1}^M \text{sign}(x + n_i)$ , the quantization error power  $E$  is

$$E = \int_{-\alpha}^{\alpha} \sum_{k=-M}^{k=M} \left( x - \frac{\alpha k}{M} \right)^2 p(x, k) dx, \quad (7)$$

where  $p(x, k)$  is the joint distribution of  $x$  and  $k$ . Furthermore, we note that  $k$  can only take on the values  $-M, -M + 2, -M + 4, \dots, M$ . Using Bayes rule and expanding the square term, we have

$$E = \int_{-\alpha}^{\alpha} \sum_{k=-M}^{k=M} \left\{ x^2 - \frac{2\alpha x k}{M} + \frac{\alpha^2 k^2}{M^2} \right\} p(k|x) p(x) dx \quad (8)$$

where  $p(k|x)$  denotes the conditional probability of  $k$  given  $x$ .  $k$  depends on the number of 1's, i.e., the number of instances in which  $x + n > 0$  for a given  $x$ . Let  $i$  be the number of 1's, hence  $j = M - i$  is the number of -1's. Since  $i + j = M$  and  $i - j = k$ , we have  $k = 2i - M$ .

Now, the variable  $i$  follows a Bernoulli distribution, whence

$$p(i|x) = \binom{M}{i} p(1|x)^i (1 - p(1|x))^{M-i},$$

where  $p(1|x)$  denotes the probability that  $\text{sign}(x + n) = 1$  with  $x \in [-\alpha, \alpha]$ . Since the noise is uniformly distributed over  $[-\beta, \beta]$ , it can easily be shown that  $p(1|x) = \frac{x+\beta}{2\beta}$ . By substituting  $k = 2i - M$  in Equation (8), we have

$$\begin{aligned} E &= \int_{-\alpha}^{\alpha} \left( \sum_{i=0}^M x^2 p(i|x) \right) p(x) dx \\ &\quad - \int_{-\alpha}^{\alpha} \left( \sum_{i=0}^M \frac{2\alpha x (2i - M)}{M} p(i|x) \right) p(x) dx \\ &\quad + \int_{-\alpha}^{\alpha} \left( \sum_{i=0}^M \frac{\alpha^2 (2i - M)^2}{M^2} p(i|x) \right) p(x) dx. \end{aligned} \quad (9)$$

The sum in the first term in the above equation is

$$\sum_{i=0}^M x^2 p(i|x) = x^2 \quad (10)$$

since  $\sum_{i=0}^M p(i|x) = 1$ . The sum in the second term of Equation (9) is

$$\begin{aligned} &\sum_{i=0}^M \frac{4\alpha x i}{M} p(i|x) - \sum_{i=0}^M 2\alpha x p(i|x) \\ &= 4\alpha x p(1|x) - 2\alpha x. \end{aligned} \quad (11)$$

The reduction is based on the observation that the first term in the Equation (11) is simply the scaled mean of a Bernoulli random variable which has the form of  $np$ . By replacing  $n =$

$M$  and  $p = p(1|x)$ , we arrive at the above results. Similarly, using the variance and mean of a Bernoulli variable [12], the sum in the third term of Equation (9) can be reduced to

$$\frac{4\alpha^2}{M^2} (Mp(1|x)(1 - p(1|x)) + (Mp(1|x))^2) - 4\alpha^2 p(1|x) + 1. \quad (12)$$

Now, by combining Equations (10), (11), (12), setting  $p(1|x) = \frac{x+\beta}{2\beta}$ ,  $p(x) = 1/2\alpha$  (uniform distribution), and performing explicit integration, we obtain the quantization error power

$$E = \frac{\alpha^2}{3} - \frac{2\alpha^3}{3\beta} + \frac{(M-1)\alpha^4}{3M\beta^2} + \frac{\alpha^2}{M} \quad (13)$$

■

## APPENDIX II PROOF OF THEOREM 4

We first calculate the variance of the transformed signal, then use Theorem 3 to obtain the desired result. The resulting bimodal-like pdf is symmetric; therefore, to determine the variance, we only need to compute one side of the integral, and multiply the result by 2. In particular, we compute the right half of the integral  $\frac{1}{\sqrt{2\pi}\delta} \int_0^\alpha x^2 e^{-\frac{(x-\alpha)^2}{2\delta^2}} dx$ . By substituting  $y = x - \alpha$ , we have

$$\begin{aligned} \frac{1}{\sqrt{2\pi}\delta} \int_0^\alpha x^2 e^{-\frac{(x-\alpha)^2}{2\delta^2}} dx &= \frac{1}{\sqrt{2\pi}\delta} \int_{-\alpha}^0 (y + \alpha)^2 e^{-\frac{y^2}{2\delta^2}} dy \\ &= \frac{1}{\sqrt{2\pi}\delta} \int_{-\alpha}^0 (y^2 + 2\alpha y + \alpha^2) e^{-\frac{y^2}{2\delta^2}} dy \\ &\approx \frac{\delta^2}{2} - \frac{\sqrt{2}\alpha\delta}{\sqrt{\pi}} (1 - e^{-\frac{\alpha^2}{2\delta^2}}) + \frac{\alpha^2}{2}, \end{aligned} \quad (14)$$

where

$\frac{1}{\sqrt{2\pi}\delta} \int_{-\alpha}^0 y^2 e^{-\frac{y^2}{2\delta^2}} dy \approx \frac{\sigma^2}{2}$  and  $\frac{1}{\sqrt{2\pi}\delta} \int_{-\alpha}^0 \alpha^2 e^{-\frac{y^2}{2\delta^2}} dy \approx \frac{\alpha^2}{2}$ , due to the fact that, for  $\delta \ll \alpha$ , the pdf is negligible outside the interval  $[-\alpha, \alpha]$ . Multiplying the right-hand side of Equation (14) by 2 to obtain the variance, and combining it with Equation (2), we obtain the desired quantization error power for the transformed signal. Since the error does not change through the SAS inverse transform, Theorem 4 is proved. ■

## CONTENTS

<b>I</b>	<b>Introduction</b>	1
<b>II</b>	<b>Related Work</b>	1
<b>III</b>	<b>RSF ADC</b>	1
<b>IV</b>	<b>RDSF ADC</b>	2
<b>V</b>	<b>Results and Discussions</b>	3
<b>VI</b>	<b>Acknowledgment</b>	4
<b>VII</b>	<b>Conclusions</b>	4

<b>References</b>		5
-------------------	--	---

<b>Appendix I: Proof of Theorem 1</b>		5
---------------------------------------	--	---

<b>Appendix II: Proof of Theorem 4</b>		6
--	--	---

## LIST OF FIGURES

1	Diagram of a stochastic flash ADC consisting of $M$ 1-bit quantizers. Uncorrelated noise is added to the input signal before quantization. The accurate output is obtained by averaging the $M$ digital outputs. . . . .	2
2	Diagram of the RDSF ADC. The input signal is transformed before feeding to the basic RSF ADC. The digital output of RSF ADC is transformed back to the correct digital signal. . . . .	2
3	(a) A Gaussian-like distribution has small variance; (b) A uniform-like distribution has medium variance; (c) A bimodal distribution has large variance. . . . .	2
4	Simulation and theoretical results on quantization error vs. std for RDSF ADC with Gaussian input signals. . . . .	4
5	Quantization error power for the quantized wavelet coefficients as a function of the number of 1-bit quantizers $M$ for (a) the Camera and (b) the Lena images. . . . .	4
6	(a) The original Camera image; (b) Original wavelet coefficients; (c) Quantized wavelet coefficients using the conventional flash ADC, and (d) Quantized wavelet coefficients using the RDSF ADC. . . . .	5